NUCL SCI TECH (2019) 30:20
https://doi.org/10.1007/s41365-019-0543-0

Preparation of amidoxime-based PE/PP fibers for extraction of uranium from aqueous solution

Xiao Xu[1,2] · Xiao-Jun Ding[2,3] · Jun-Xuan Ao[2,3] · Rong Li[2] · Zhe Xing[2] · Xi-Yan Liu[2] · Xiao-Jing Guo[2] · Guo-Zhong Wu[2] · Hong-Juan Ma[2] · Xiao-Yan Zhao[1]

Received: 19 March 2018 / Revised: 13 June 2018 / Accepted: 11 July 2018 / Published online: 17 January 2019

Abstract A novel amidoxime-based fibrous adsorbent, denoted as PE/PP-*g*-(PAAc-*co*-PAO), was prepared by pre-irradiation grafting of acrylic acid and acrylonitrile onto polyethylene-coated polypropylene skin–core (PE/PP) fibers using ^{60}Co γ-ray irradiation, followed by amidoximation. The original and modified PE/PP fibers were characterized by a series of characterization methods to demonstrate the attachment of amidoxime groups onto the PE/PP fibers. Breaking strength tests confirmed that the fibrous adsorbent could maintain good mechanical properties. The adsorption capacity of the PE/PP-*g*-(PAAc-*co*-PAO) fibers was investigated in simulated seawater with an initial uranium concentration of 330 μg/L. The uranium adsorption capacity was 2.27 mg/g-adsorbent after 24 h in simulated seawater, and the equilibrium data were well described by the Freundlich isotherm model. The PE/PP-*g*-(PAAc-*co*-PAO) adsorbent exhibited good regeneration and recyclability during five adsorption–desorption cycles. The adsorption test was also performed in simulated radioactive effluents with uranium concentrations of 10 and 100 μg/L. The effect of the pH value on the adsorption capacity was also studied. At a very low initial concentration 10 μg/L solution, the PE/PP-*g*-(PAAc-*co*-PAO) fiber could remove as much as 93.0% of the uranium, and up to 71.2% of the uranium in the simulated radioactive effluent. These results indicated that the PE/PP-*g*-(PAAc-*co*-PAO) adsorbent could be used in radioactive effluents over a wide range of pH values. Therefore, the PE/PP-*g*-(PAAc-*co*-PAO) fibers, with their high uranium selectivity, good regeneration and recyclability, good mechanical properties, and low cost, are promising adsorbents for extracting uranium from aqueous solutions.

Keywords Amidoxime groups · Pre-irradiation · PE-coated PP skin–core fiber · Adsorption · Uranium

1 Introduction

Uranium is the main source of fuel for nuclear power generation, which is considered to be one of the most environmentally friendly energy sources [1]. With the rapid development of nuclear power, the demand for uranium fuel continues to increase. Although terrestrial ores are still usable, the content of uranium in the ore (i.e., the grade) will decrease over time, requiring more adsorption materials to be processed to accomplish the necessary reserves [2]. The amount of uranium in the oceans is thousands of times greater than the amount in terrestrial ores [3]. Therefore, uranium in seawater will be a near-limitless resource for nuclear fuel in the future, and its recovery will avoid the deleterious effects of terrestrial mining on the

This work was supported by the National Natural Science Foundation of China (Nos. U1732151 and 21676291) and Strategic Pilot and Technology Special Funds of the Chinese Academy of Science (No. XDA02030200).

✉ Hong-Juan Ma
mahongjuan@sinap.ac.cn

✉ Xiao-Yan Zhao
zhaoxiaoyan@cczu.edu.cn

[1] School of Petrochemical Engineering, Changzhou University, Changzhou 213164, China

[2] Shanghai Institute of Applied Physics, Chinese Academy of Sciences, Shanghai 201800, China

[3] University of Chinese Academy of Sciences, Beijing 100049, China

environment [4]. Although there is a large amount of uranium in natural seawater, the concentration of uranium is very low (3.3 μg/L), while the concentrations of other metal ions in seawater are relatively high [5, 6], which makes it a great challenge to economically extract uranium from seawater. Therefore, the extraction of such low concentrations of uranium requires advanced adsorbents that have high capacity and selectivity for uranium in seawater.

Additionally, with the rapid development of the nuclear energy industry, a large amount of low-level radioactive wastewater will be discharged from the nuclear industry, especially from nuclear power plants. Because of its alpha radiation, uranium is considered a toxic and radioactive ion [7]. High contents of uranium in soil and water lead to its transfer to the food chain and then to human tissues [8, 9]. Hence, the removal of uranium from radioactive effluents has also attracted worldwide attention.

At present, there are a variety of methods for uranium extraction [1, 10, 11], including ion exchange, flotation, solvent extraction, and adsorption [12–16]. Since the 1960s, adsorption has drawn considerable attention for its many potential advantages, such as moderate operation, cost-effectiveness, and low emissions. Therefore, it is a highly promising method for uranium extraction from seawater [17–21]. Driven by ocean currents, fibrous adsorbent is the only materials that can be deposited in the ocean like kelp and seaweed, without additional driving force for natural adsorption. With the advantages of easy placement and salvage, fibrous adsorbents are the only materials with practical applications [22].

Amidoxime-based fibrous adsorbents have been widely studied in recent decades for the extraction of uranium from seawater, which takes advantage of their high uranium adsorption capacities [23–27]. Japanese researchers have prepared adsorbents by the radiation-induced grafting of acrylonitrile onto PE non-woven fabric and the conversion of the cyano groups into amidoxime (AO) groups for the extraction of uranium from seawater [28, 29]. Furthermore, adsorption by chelating polymers is the most promising approach for uranium recovery from seawater, compared to other separation methods such as coprecipitation, coagulation, and membrane filtration [30–32], and adsorbents containing AO functional groups are the most promising adsorbents [28, 32].

Recently, American researchers have synthesized a class of fibrous materials with a higher adsorption capacity by increasing the specific surface area and grafting rate. The optimum adsorption capacity could reach 3.3 mg/g after adsorption in seawater for 43 days [33, 34]. Nevertheless, the cost of extracting uranium from seawater using the best adsorbents in the USA and Japan is still higher than that of land-based uranium mining. Therefore, we need to focus on the development of materials with better performances.

In this work, aiming to meet the requirements of high adsorption capacity, high uranium selectivity, good mechanical properties, and low cost, commercial PE-coated PP skin–core fibers (PE/PP) were used as substrate materials for the preparation of amidoxime-based polymer fibrous adsorbents for the first time. The price of PE/PP fibers is lower than that of our previous substrate material, ultra-high molecular weight polyethylene (UHMWPE) fibers. The mechanical properties of PE/PP fibers are similar to those of commercial fibers available in the market that can be used for adsorption in seawater and radioactive effluents. The adsorbents were prepared by the relatively low absorbed dose pre-irradiation-induced co-graft polymerization of polyacrylonitrile (PAN) and polyacrylic acid (PAAc) followed by amidoximation. The effects of the absorbed dose, monomer concentration, grafting temperature, and grating time were investigated to determine the optimal conditions for grafting. The modified PE/PP fibers were characterized in detail by Fourier transform infrared spectrometry (FT-IR), X-ray photoelectron spectroscopy (XPS), scanning electron microscopy (SEM), thermogravimetric analysis (TGA), and the single-filament tensile test. The results from the FT-IR, XPS, and SEM analyses indicated that the grafting of acrylonitrile (AN) and acrylic acid (AAc) onto the PE/PP fibers was successful. The TGA and breaking force tests showed that the PE/PP-*g*-(PAAc-*co*-PAO) had good thermal stability and mechanical properties. Then, the PE/PP-*g*-(PAAc-*co*-PAO) adsorbent was used to extract uranium from aqueous solution, and the effects of the pH value, initial concentration, contact time, and coexisting ions of the solution were discussed in detail. Batch experiments in simulated seawater and simulated radioactive effluent were conducted, and the results suggested that the PE/PP-*g*-(PAAc-*co*-PAO) adsorbent could be used to extract uranium from seawater and remove uranium from radioactive effluents.

2 Materials and experimental methods

2.1 Materials

PE-coated PP skin–core fiber (PE/PP) was supplied by Haining Xin Gao Fibers Co., Ltd. Acrylonitrile (AN), acrylic acid (AAc), *N*,*N*-dimethylformamide (DMF), sodium carbonate (Na_2CO_3), hydroxylamine hydrochloride ($NH_2OH{\cdot}HCl$), sodium hydroxide (NaOH), hydrochloric acid (HCl), and dimethyl sulfoxide (DMSO) were purchased from Sinopharm Chemical Reagent Company and used as received. The 1000 ppm standard solutions of uranium and competing ions were purchased from SPEX Certi Prep, Inc. Nitrogen (99.99%) gas was obtained from Shanghai Luoyang Gas Canned Co., Ltd.

2.2 Manufacturing of the PE/PP fibrous adsorbent

The preparation scheme for the PE/PP-*g*-(PAAc-*co*-PAO) fibers is outlined in detail in Fig. 1. (1) AAc and AN were grafted onto the PE/PP fibers by pre-irradiation-induced graft polymerization; (2) the amidoximation of the PE/PP-*g*-(PAAc-*co*-PAN) fibers by reaction with hydroxylamine hydrochloride was carried out to prepare the PE/PP-*g*-(PAAc-*co*-PAO) fibers.

The PE/PP fibers were pre-irradiated with ^{60}Co γ-rays at room temperature in air over the range of 50–200 kGy. Then, the irradiated fibers were immersed in a flask containing an AAc/AN/DMF solution. Before the irradiated fibers were placed into the AAc/AN/DMF solution in a water bath at the specified temperature for the specified grafting time, the solution was bubbled with nitrogen for 20 min. After grafting, the PE/PP-*g*-(PAAc-*co*-PAN) fibers were washed with DMF to remove any remaining monomers and homopolymers and dried. The degree of grafting (D_g) was calculated as follows:

$$D_g(\%) = \frac{M_2 - M_1}{M_1} \times 100, \quad (1)$$

where M_1 is the weight of the original PE/PP fiber and M_2 is the weight of the PE/PP-*g*-(PAAc-*co*-PAN) fiber.

Finally, a 5 wt% solution of NH_2OH HCl was prepared with 50/50 (v/v)% deionized water/DMSO, and the pH of the solution was adjusted to neutral with Na_2CO_3. The PE/PP-*g*-(PAAc-*co*-PAN) fibers were reacted with the 5 wt% solution of $NH_2OH{\cdot}HCl$ at 70 °C for 4 h to convert the nitrile groups into AO groups. After amidoximation, the modified fiber PE/PP-*g*-(PAAc-*co*-PAO) was washed with deionized water and then dried in a vacuum oven at 60 °C. The AO group density of the PE/PP-*g*-(PAAc-*co*-PAO) fiber was determined using the following equation:

$$\text{AO Density (mmol/g)} = \frac{1000 \times (W_i - W_0)}{33\, W_i}, \quad (2)$$

where W_0 and W_i are the weights of the PE/PP-*g*-(PAAc-*co*-PAN) and PE/PP-*g*-(PAAc-*co*-PAO) fibers; 33 is the molecular weight of the AO group minus the molecular weight of the nitrile group.

2.3 Characterization of the modified fibers

The compositions and structures of the fiber samples were characterized by FT-IR (Thermo Nicolet Company, USA), XPS (Thermo SCIENTIFIC ESCALAB 250Xi Instrument, USA), and thermogravimetric analysis (PerkinElmer, USA). A scanning electron microscope (JSM-6700F, JEOL, Japan) was used to investigate the surface morphology of the fiber samples. The BET surface area was obtained through nitrogen absorption–desorption measurements using a surface aperture adsorption instrument (ASAP2010C, Micromeritics, USA). The breaking strength of the fiber samples was tested using a tension instrument (LLY-06E, Laizhou Electron Instrument Co. Ltd. China). In addition, the concentrations of the metal ions in the simulated seawater and the aqueous solution were determined by inductively coupled plasma atomic emission spectrometry (ICP-AES, PerkinElmer Optima 8000) and inductively coupled plasma mass spectrometry (ICP-MS, PerkinElmer, NexION 300D), respectively.

2.4 Uranium sorption by the PE/PP-*g*-(PAAc-*co*-PAO) fibers

2.4.1 Simulated seawater for the rapid adsorption test

For the simulated seawater adsorption experiment, the initial concentrations of uranium and the competing metal ions in the simulated seawater were about 100 times as

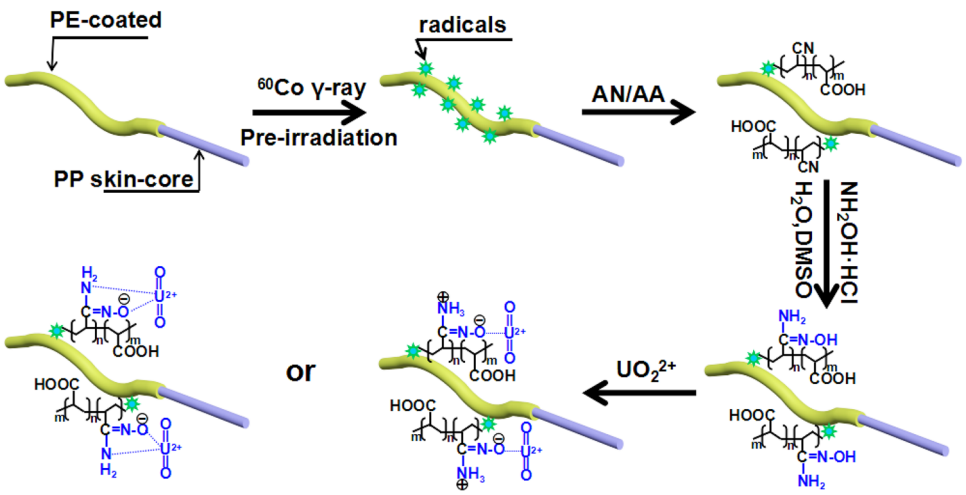

Fig. 1 (Color online) Schematic representation of the preparation of the PE-coated PP skin–core fiber (PE/PP) adsorbent containing grafted chains with amidoxime groups

high as those found in natural seawater (Table 1). The pH value was adjusted to 8.0 by adding a small amount of Na_2CO_3. 0.1 g of PE/PP-*g*-(PAAc-*co*-PAO) fibers was placed into 5 L of simulated seawater, and the adsorption experiment was implemented on a rotary shaker at 25 °C and 100 rpm for different contact times [35]. At the specified time interval (1, 3, 6, 14, 24, 32, 45, and 50 h), the sample was taken out, digested, and analyzed using ICP-AES.

The adsorption capacity of the PE/PP-*g*-(PAAc-*co*-PAO) fibers for metal ions can be determined by using the following equation:

$$Q = CV/W, \tag{3}$$

where Q (mg/g) is the adsorption capacity of the PE/PP-*g*-(PAAc-*co*-PAO) fibers for metal ions, C (mg/L) is the concentration of the measured metal ion as determined by ICP-AES, V (L) is the practical digested solution volume, and W (g) is the weight of the dried PE/PP-*g*-(PAAc-*co*-PAO) fiber used.

2.4.2 Adsorption isotherms

The adsorption isotherms were investigated by the batch technique. About 10 mg of dried PE/PP-*g*-(PAAc-*co*-PAO) fibers was placed into 100 mL of uranium solutions with initial concentrations ranging from 2 to 25 mg/L [37]. The adsorption solutions were shaken at 100 rpm at 25 °C for 12 h. The uranium concentrations in the solution were determined by ICP-AES, and the uranium adsorption capacity was calculated using Eq. (5).

$$Q_e = \frac{(C_0 - C_e) \times 0.1}{W}, \tag{4}$$

where C_0 and C_e are the initial and equilibrium concentrations of uranium (mg/L) measured by ICP-MS, respectively, and 0.1 (L) is the volume of the uranium solution.

2.4.3 Simulated radioactive effluent adsorption

The adsorption capacity of PE/PP-*g*-(PAAc-*co*-PAO) in simulated radioactive effluent was measured using low initial concentrations of uranium in aqueous solutions containing sodium fluoride (NaF). The adsorption experiments were performed in 100-mL plastic bottles, which were placed in a rotary shaker at 25 °C and 100 rpm for 24 h. More specifically, 20 mg of the PE/PP-*g*-(PAAc-*co*-PAO) adsorbent, 30 g/L of NaF, and uranium solutions with an initial concentration of 10 or 100 μg/L were added to the plastic bottles, and then HNO_3 and NaOH solutions were used to adjust the pH value of the solution. Afterward, the plastic bottles were placed in a rotary shaker at 25 °C and 100 rpm for 24 h. The removal ratio (R) of uranium was evaluated as follows:

$$R\,(\%) = \frac{C_0 - C_e}{C_0} \times 100, \tag{5}$$

where C_0 and C_e are the initial and equilibrium concentrations of uranium (mg/L) measured by ICP-MS, respectively.

3 Results and discussion

3.1 Radiation grafting of AAc and AN onto the PE/PP fibers

The preparation of PE/PP-*g*-(PAAc-*co*-PAN) fibers takes advantage of the different effects of radiation on the shell PE layer and core PP layer of the fibers [36]. Adsorption applications require an adsorbent with a *D*g of 100–150% and an appropriate density and utilization percentage of functional groups. Accordingly, the effects of the absorbed dose, reaction time, reaction temperature, and monomer concentration on the *D*g of the PE/PP-*g*-(PAAc-*co*-PAN) fibers were investigated, as shown in Fig. 2. The PE/PP fibers were irradiated at different absorbed doses from 0 to 200 kGy to investigate the effects of the absorbed dose on the *D*g of the PE/PP-*g*-(PAAc-*co*-PAN) fibers. The *D*g of AAc and AN increased linearly with the increase in the absorbed dose and reached 107.5% at 80 kGy (with 60 vol% monomer concentration, and at 50 °C after grafting for 5 h). As shown in Fig. 2a, the *D*g of the PE/PP-*g*-(PAAc-*co*-PAN) fibers increased slightly when the

Table 1 Concentration of ions in simulated seawater

Element	U	V	Fe	Co	Ni	Cu	Zn	Pb	Mg	Ca
Ions	$UO_2(CO_3)_3^{4-}$ $UO_2(CO_3)_2^{2-}$	$VO_2(OH)_3^{2-}$ VO_3^- HVO_4^{2-} $H_2VO_4^-$	F^{3+}	Co^{2+}	Ni^{2+}	Cu^{2+}	Zn^{2+}	Pb^{2+}	Mg^{2+}	Ca^{2+}
Concentration (μg/L)	330	152	141	5.3	101	65	408	34.6	1.2×10^5	0.6×10^5

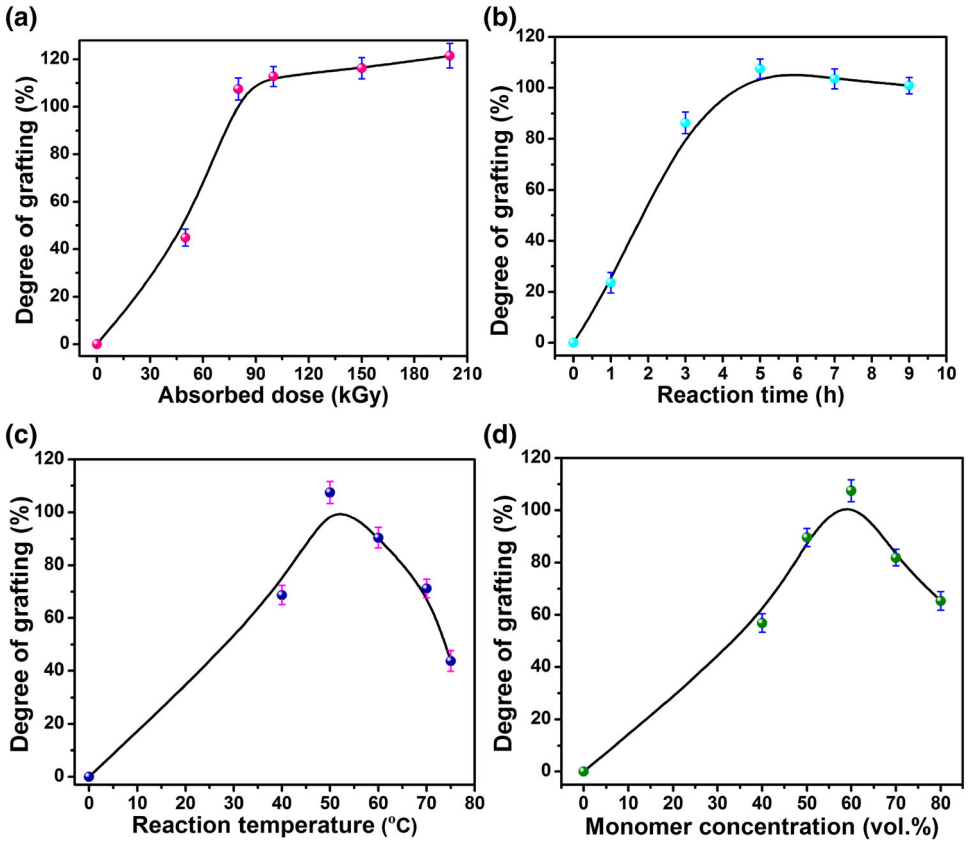

Fig. 2 (Color online) D_g of the PE/PP-*g*-(PAAc-*co*-PAN) fibers as a function of **a** absorbed dose, **b** reaction time, **c** reaction temperature, and **d** monomer concentration

absorbed dose was higher than 80 kGy, which indicated that 80 kGy was the optimal absorbed dose from the point of view of energy consumption and the maintenance of mechanical properties. The *D*g of AAc and AN increased linearly with the increase in reaction time and reached saturation after 5 h (with 80 kGy absorbed dose and 60 vol% monomer concentration at 50 °C) as shown in Fig. 2b. The effects of the reaction temperature on the degree of grafting are shown in Fig. 2c (with 80 kGy absorbed dose, and 60 vol% monomer concentration after grafting for 5 h). The *D*g of the PE/PP-*g*-(PAAc-*co*-PAN) fibers increased as the reaction temperature increased up to 50 °C. At 0–60 vol% monomer concentration, the *D*g of AAc and AN increased linearly with the increase in the monomer concentration (with 80 kGy absorbed dose, and at 50 °C after grafting for 5 h) as shown in Fig. 2d. The results showed that a great deal of homopolymers were produced at higher absorbed dose, reaction temperature, and monomer concentration, thus preventing the diffusion of AAc and AN to the interface of the PE/PP fibers.

Taking into account the radiation damage, energy consumption, and the mechanical properties of the fibers after treatment, the absorbed dose of 80 kGy, a reaction time of 5 h, reaction temperature of 50 °C, and monomer concentration of 60 vol% were identified as the optimum conditions and exploited for the preparation of the PE/PP-*g*-(PAAc-*co*-PAN) fibers, which exhibited a D_g of 107.5% when prepared using these conditions. After the amidoximation modification, the AO group density of the PE/PP-*g*-(PAAc-*co*-PAO) fibers was 6.8 mmol/g, which was suitable for applications in metal ion adsorption [18].

3.2 Characterization of the pristine and modified PE/PP fibers

3.2.1 FT-IR characterization

The FT-IR spectra of the (a) PE/PP, (b) PE/PP-*g*-(PAAc-*co*-PAN), and (c) PE/PP-*g*-(PAAc-*co*-PAO) fibers are shown in Fig. 3. The characteristic adsorption bands at 2916 and 2848 cm^{-1} were attributed to the asymmetric and symmetric stretching of the $–CH_2–$ groups, and also appeared in the modified samples [37]. In the spectrum of the PE/PP-*g*-(PAAc-*co*-PAN) fibers, new peaks were observed at 1715 cm^{-1}, corresponding to the adsorption peak of –COOH in PAAc. These new features revealed that acrylic acid was successfully grafted onto the PE/PP fibers. Additionally, a sharp peak at 2245 cm^{-1} was assigned as $–C\equiv N–$ from the successful grafting of AN onto the PE/PP fibers. In the spectrum of the PE/PP-*g*-(PAAc-*co*-PAO) fibers, new characteristic peaks for N–H and O–H, –C=N–, and –N–O– appeared at 3000 to 3600, 1649, and 920 cm^{-1},

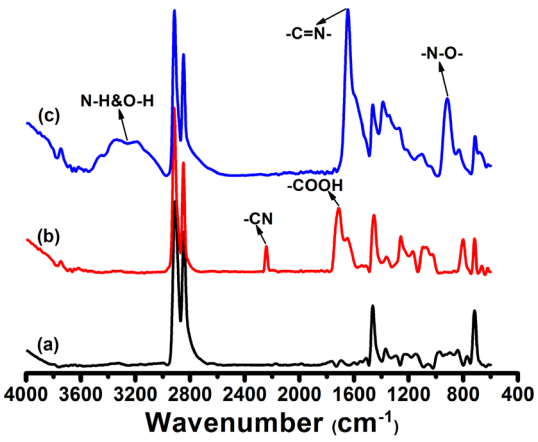

Fig. 3 (Color online) FT-IR spectra of the **a** PE/PP, **b** PE/PP-*g*-(PAAc-*co*-PAN), and **c** PE/PP-*g*-(PAAc-*co*-PAO) fibers

respectively. Meanwhile, the peak at 2245 cm^{-1} related to –C≡N–disappeared and the –C=N– peak increased sharply, indicating that the nitrile group was transformed into the AO group after reaction with hydroxylamine hydrochloride [1].

3.2.2 XPS characterization

XPS analysis was carried out as shown in Fig. 4. As shown in Fig. 4a, a strong peak attributed to C 1s (284.7 eV) was observed in the XPS spectrum of the pristine PE/PP. After graft modification, two new peaks emerged at 399.6 (N 1s) and 531.7 eV (O 1s) in both PE/PP-*g*-(PAAc-*co*-PAN) and PE/PP-*g*-(PAAc-*co*-PAO). Characteristic peaks appeared at 381.2 eV (U 4f) after PE/PP-*g*-(PAAc-*co*-PAO) adsorbed uranium. Further analysis of the C 1s spectrum of the PE/PP-*g*-(PAAc-*co*-PAO) fibers was performed as shown in Fig. 4b, and four peaks at 284.9, 285.7, 286.7, and 288.0 eV could be observed, which could be assigned to C–C, C–O/N, C=N, and O=C–O groups, respectively [38]. As for the N 1s spectrum of the PE/PP-*g*-(PAAc-*co*-PAO) fibers, there were two peaks at 399.5 and 400.4 eV in Fig. 4c, indicating that C=N and C–N groups were introduced, which was consistent with the C 1s region. In short, these results demonstrated that the amidoxime and carboxylic acid functional groups can coexist and revealed that PE/PP-*g*-(PAAc-*co*-PAO) fibers that might provide available binding sites for uranium adsorption were successfully synthesized.

3.2.3 SEM and BET characterization

SEM images of the pristine and modified PE/PP fibers were obtained to compare their physical appearance and to explore whether any damage to the fibers occurred during the grafting and modification processes, as shown in Fig. 5. For the pristine PE/PP fibers, the surface was relatively rough (Fig. 5A and a). After grafting AAc and AN, the morphology of the PE/PP-*g*-(PAAc-*co*-PAN) fibers was relatively smooth, and additionally, the diameter of the fiber increased significantly. The increased diameter should be attributed to the grafted AAc and AN chains, indicating that AAc and AN were successfully grafted onto the PE/PP fibers (Fig. 5B and b). After amidoximation, the surface of the PE/PP fibers was wrapped in amidoxime gel, and the compatibility between the hydrophilic PAO chains and the hydrophilic PAAc chains made the surface of the fiber smoother (Fig. 5C and c) [39]. Additionally, the diameter of the fibers enlarged gradually after each chemical reaction, especially after the graft polymerization process. Therefore, the diameter of the PE/PP-*g*-(PAAc-*co*-PAN) fibers increased very obviously compared to that of the pristine PE/PP fibers. The average values of the diameters of the pristine PE/PP fibers, PE/PP-*g*-(PAAc-*co*-PAN) fibers, and PE/PP-*g*-(PAAc-*co*-PAO) fibers were 12.4 ± 0.08, 16.8 ± 0.06, and 17.5 ± 0.08 μm, respectively. Due to the use of a low absorption dose in the process of pre-irradiation graft polymerization, there was no visible damage to the PE/PP fibers.

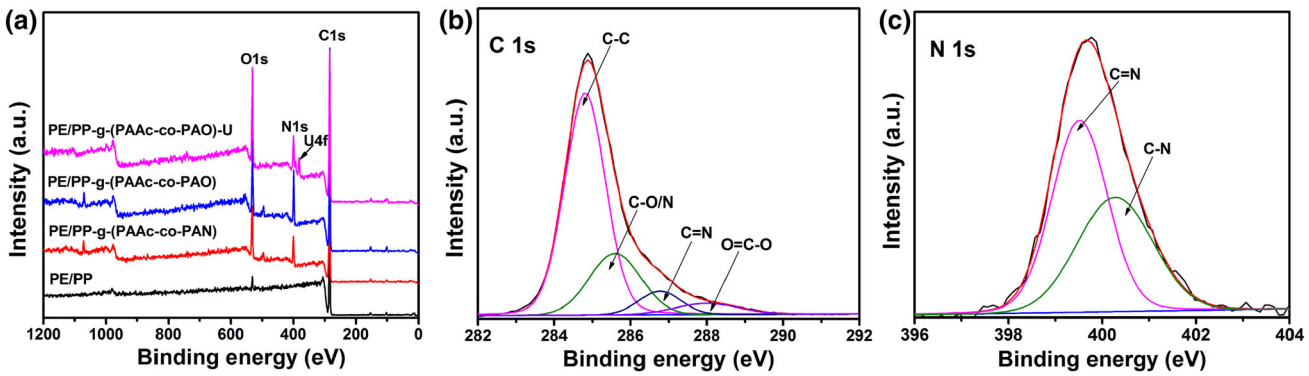

Fig. 4 (Color online) The XPS survey spectra of PE/PP, PE/PP-*g*-(PAAc-*co*-PAN), PE/PP-*g*-(PAAc-*co*-PAO), and PE/PP-*g*-(PAAc-*co*-PAO)-U fibers: **a** overall spectrum, **b** the C 1s spectrum of PE/PP-*g*-(PAAc-*co*-PAO), and **c** the N 1s spectrum of PE/PP-*g*-(PAAc-*co*-PAO)

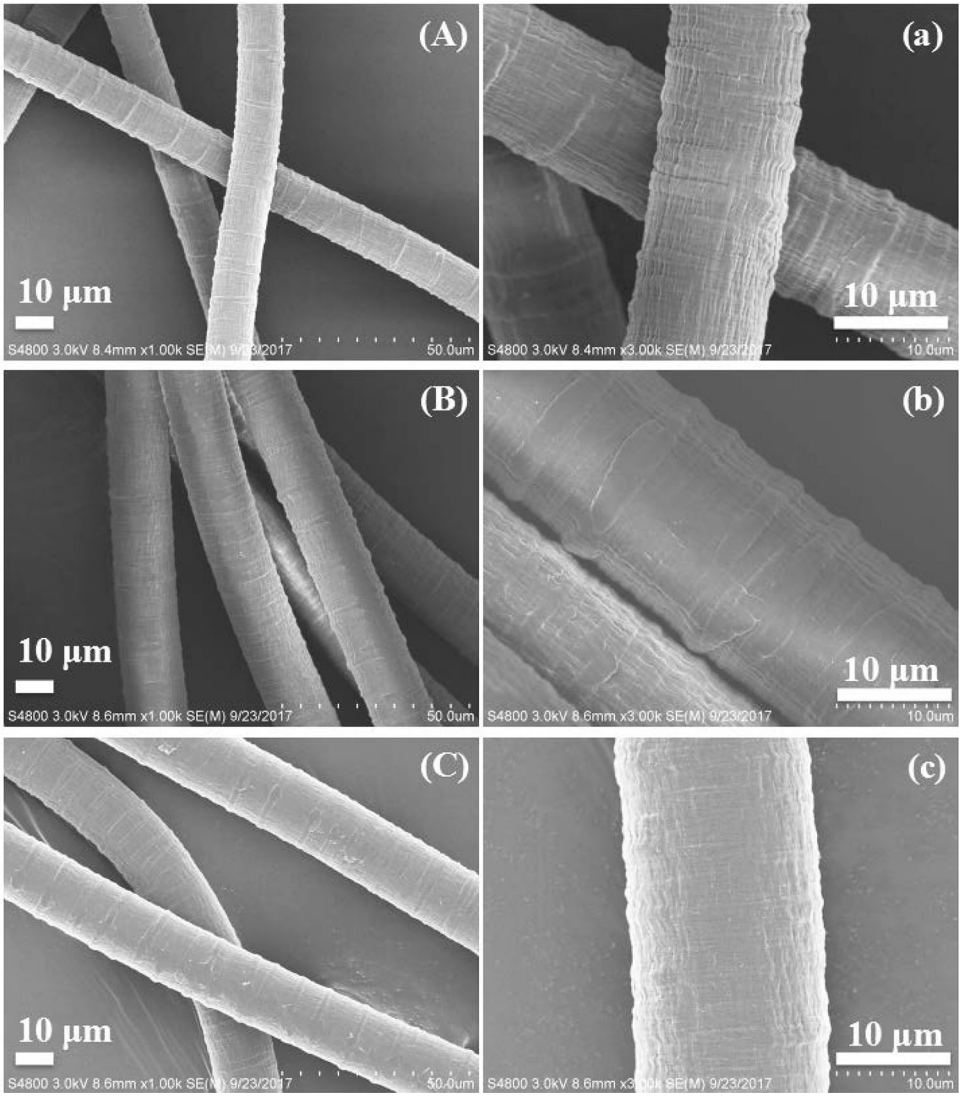

Fig. 5 SEM images of PE/PP (**A** and **a**), PE/PP-*g*-(PAAc-*co*-PAN) (**B** and **b**), and PE/PP-*g*-(PAAc-*co*-PAO) (**C** and **c**) fibers

The N_2 adsorption–desorption test (BET method) revealed that the BET surface area of the PE/PP fiber reached 4.3 m^2/g, and that of the PE/PP-*g*-(PAAc-*co*-PAN) fiber reached 3.7 m^2/g, which implied that the PE/PP fibers were relatively rough compared to the PE/PP-*g*-(PAAc-*co*-PAN) fibers. Compared to the BET surface area of the PE/PP fibers, that of the PE/PP-*g*-(PAAc-*co*-PAO) fibers reached 6.4 m^2/g, representing an increase of 48.8%, which implied that increasing the specific surface area will facilitate the extraction of uranium from aqueous solutions [26].

Combining the FT-IR, XPS, and SEM analyses, it can be concluded that a remarkable change took place in the chemical composition and microstructure of the PE/PP-*g*-(PAAc-*co*-PAO) fibers compared to those of the pristine PE/PP fibers, which indicated that the PE/PP-*g*-(PAAc-*co*-PAO) fibers were endowed with new properties.

3.2.4 Thermogravimetric analysis

The TGA and DTG curves of the original PE/PP, PE/PP-*g*-(PAAc-*co*-PAN), and PE/PP-*g*-(PAAc-*co*-PAO) fibers are shown in Fig. 6. The maximum thermal degradation rate of the pure PE/PP fibers occurred at 465 °C, and no residue remained at 496 °C. Meanwhile, four decomposition processes of the PE/PP-*g*-(PAAc-*co*-PAN) fibers appeared with maximum decomposition rate temperatures of about 240, 294, 374, and 498 °C [40]. The TGA curve showed that the weight loss ratio of decarboxylation was much lower than that of the carbonization of the PAN chains. The results revealed that most of the grafted copolymer molecular chains consisted of the AN molecular chain. After amidoximation, the PE/PP-*g*-(PAAc-*co*-PAO) fibers became less thermally stable compared to the PE/PP-*g*-(PAAc-*co*-PAN) fibers and began to degrade at about 182 °C. In general, although the thermal stability of the

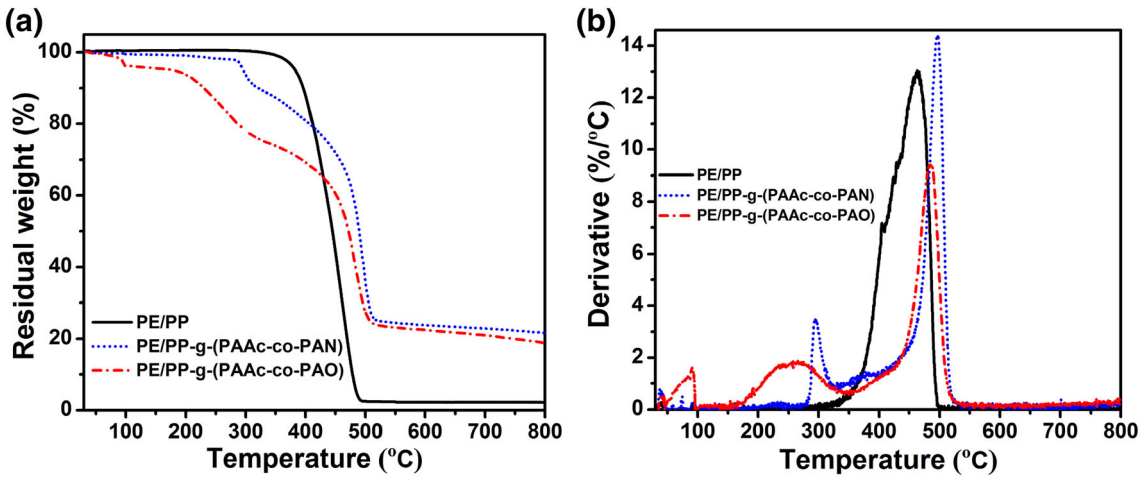

Fig. 6 (Color online) TGA (**a**) and DTG (**b**) curves of PE/PP fibers, PE/PP-*g*-(PAAc-*co*-PAN) fibers, and PE/PP-*g*-(PAAc-*co*-PAO) fibers in an N_2 atmosphere

fibers declined gradually during the modification process, that of the PE/PP fiber remained unchanged after graft modification. The chemical and thermal stability of the main chain indicates that the modified fibers can be used for adsorption in the natural environment.

3.2.5 Mechanical performance test

The breaking strength of the pristine and pre-irradiated PE/PP, PE/PP-*g*-(PAAc-*co*-PAN), and PE/PP-*g*-(PAAc-*co*-PAO) fibers is shown in Fig. 7. The breaking strength of the pristine PE/PP fiber was more than 3.53 cN. After pre-irradiation at an absorbed dose of 80 kGy, the breaking strength was reduced to 1.96 cN, which may be attributed to radiation-induced degradation and cross-linking of the PE/PP molecular chain [18]. The PE/PP-*g*-(PAAc-*co*-PAN) fiber exhibited a higher breaking strength of 2.03 cN than the PE/PP fiber pre-irradiated with 80 kGy. A potential reason for the increase in the breaking strength of the PE/PP-*g*-(PAAc-*co*-PAN) fiber might be that the thick grafted layer on the surface of the PE/PP fiber shared part of the stress. The breaking strength of the PE/PP-*g*-(PAAc-*co*-PAO) fiber was about 2.11 cN, indicating that amidoximation had no influence on the breaking strength of the PE/PP fiber pre-irradiated at 80 kGy. These results demonstrated that radiation damage was the main reason for the loss of the mechanical properties of the fiber, while the chemical reactions had little effect. Generally, fibers with a breaking strength of 2.11 cN can withstand ocean currents and can be used for uranium extraction from seawater and in other environmental remediation applications [39].

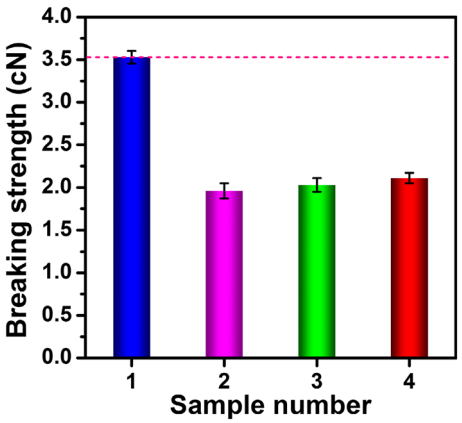

Fig. 7 (Color online) Plot of the breaking strength of the (1) PE/PP fiber, (2) PE/PP fiber pre-irradiated with 80 kGy, (3) PE/PP-*g*-(PAAc-*co*-PAN) fiber, and (4) PE/PP-*g*-(PAAc-*co*-PAO) fiber

3.3 Uranium adsorption tests in simulated seawater

At the ultralow uranium concentration of 3.3 μg/L found in seawater, it would take months to reach adsorption equilibrium. In order to screen for excellent adsorbents, simulated seawater with an initial concentration 100 times higher than that of natural seawater was used in the adsorption test. As can be seen from Fig. 8, the uranium adsorption capacity of the PE/PP-*g*-(PAAc-*co*-PAO) fiber reached 2.27 mg/g-adsorbent after 24 h, which was greater than the reported amount of uranium adsorbed by AO-PAN fibers (about 0.3 mg/g-adsorbent) [19] and a nano-adsorbent (1.6 mg/g-adsorbent) [20]. According to the results, the selectivity of the PE/PP-*g*-(PAAc-*co*-PAO) fibers followed the order Mg > Zn > Ca > U > Fe > V > Ni > Cu > Pb > Co, which indicated that the PE/PP-*g*-(PAAc-*co*-PAO) fibers showed good adsorption selectivity against almost all of the ions except for the zinc, magnesium, and calcium ions. A possible cause is that the concentrations of zinc, magnesium, and calcium ions in simulated seawater were much higher than that of uranium, and that the –

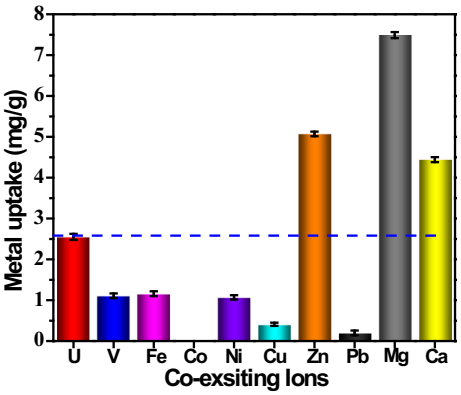

Fig. 8 (Color online) Adsorption capacities of the PE/PP-*g*-(PAAc-*co*-PAO) fibers for uranium and coexisting ions in simulated seawater

COOH group of the PE/PP-*g*-(PAAc-*co*-PAO) fibers had a stronger affinity with zinc, magnesium, and calcium ions. However, the recovery of uranium will be carried out by elution, and zinc, magnesium, and calcium ions can be easily eluted with a low concentration of hydrochloric acid (HCl). When uranium is extracted, vanadium is deemed to be the most important competitive ion, as the elution of vanadium requires a very high concentration of acid, which can damage the fibrous adsorbent [41]. The results showed that the adsorption capacity for uranium was higher than that for vanadium.

In order to determine the equilibrium time for maximum uptake, the uranium adsorption kinetics were examined by soaking 0.1 g of PE/PP-*g*-(PAAc-*co*-PAO) fibers in simulated seawater (pH 8.0, 5 L). Figure 9 shows the capacities of PE/PP-*g*-(PAAc-*co*-PAO) fibers for the metal ions as functions of contact time. According to the results, the PE/PP-*g*-(PAAc-*co*-PAO) fibers reached adsorption balance after 50 h with a capacity of 2.94 mg/g-adsorbent, and their Ni, Cu, and Pb adsorption capacities were 1.20, 0.56, and 0.23 mg/g-adsorbent after 32 h in simulated seawater, respectively, after which they remained almost unchanged with further contact time. In addition, the PE/PP-*g*-(PAAc-*co*-PAO) fibers had almost no adsorption capacity for Co.

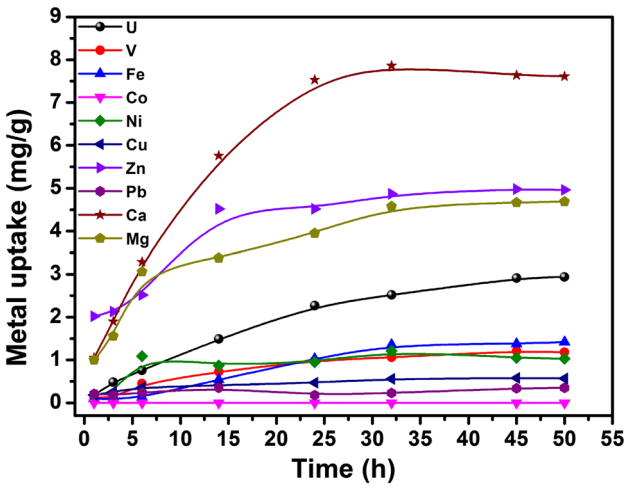

Fig. 9 (Color online) The adsorption kinetics of the PE/PP-*g*-(PAAc-*co*-PAO) fibers in simulated seawater

3.4 Reusability of the PE/PP-*g*-(PAAc-*co*-PAO) adsorbent

It is important for an effective and economical adsorbent to be easily regenerable and reusable. The adsorption–desorption experiment was carried out for five cycles in simulated seawater. A 0.5 M HCl solution (at room temperature for 2 h) was used as the eluent, and a 5 mM sodium hydroxide (NaOH) solution (at room temperature for 5 min) was used for regeneration [42].

The reusability of PE/PP-*g*-(PAAc-*co*-PAO) adsorbents was investigated over five adsorption–desorption cycles, and the adsorption capacities are shown in Fig. 10. The PE/PP-*g*-(PAAc-*co*-PAO) adsorbent showed no loss of uranium adsorption capacity after 3 consecutive cycles under simulated seawater conditions. Compared to the first adsorption, the recycled PE/PP-*g*-(PAAc-*co*-PAO) adsorbent exhibited a 3.5% and 5.3% loss of uranium adsorption capacity in the fourth and fifth adsorption cycles, respectively. These results implied that PE/PP-*g*-(PAAc-*co*-PAO) adsorbent could be easily and effectively regenerated as an efficient adsorbing material for the extraction of uranium from seawater.

3.5 Adsorption isotherms

The adsorption isotherm is illustrated in Fig. 11. The linearized Langmuir and Freundlich models are often

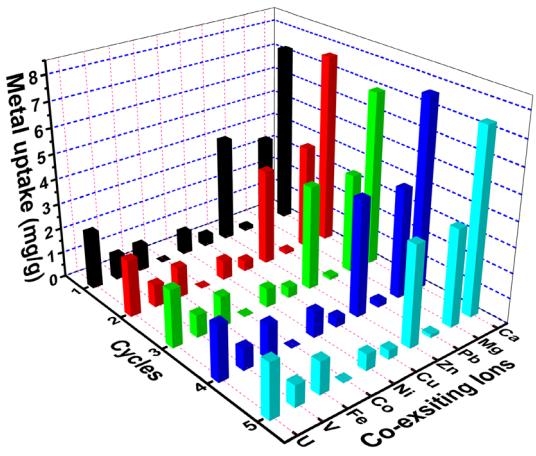

Fig. 10 (Color online) Performance of PE/PP-*g*-(PAAc-*co*-PAO) over five regeneration cycles in the adsorption of uranium with an initial concentration of 330 μg/L and coexisting ions from simulated seawater

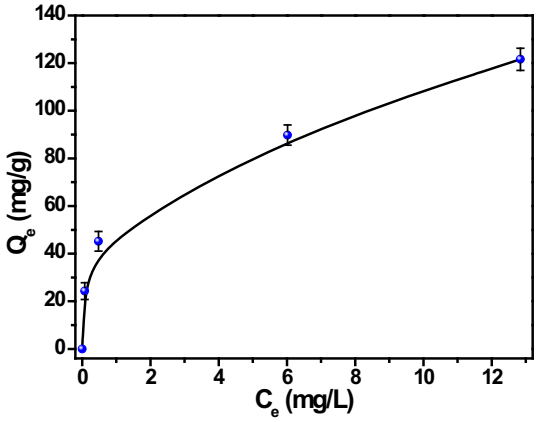

Fig. 11 Adsorption isotherm of the PE/PP-*g*-(PAAc-*co*-PAO) adsorbent for uranium (10 mg of PE/PP-*g*-(PAAc-*co*-PAO) fibers, retention time 12 h, pH 6.0, T = 25 °C, and V = 100 mL)

selected to describe equilibrium adsorption isotherms. The Langmuir equation is given as:

$$\frac{C_e}{Q_e} = \frac{1}{K_L Q_m} + \frac{C_e}{Q_m}, \tag{6}$$

where Q_e (mg/g) is the uranium adsorption capacity at the equilibrium concentration, Q_m is the maximum adsorption capacity (mg/g), and K_L is the Langmuir constant. The Freundlich equation is defined as:

$$\lg Q_e = \lg K_F + \frac{1}{n} \lg C_e, \tag{7}$$

where K_F ((mg/g) (L/mg)$^{1/n}$) and n are the Freundlich constants, which represent the adsorption capacity and the adsorption intensity, respectively.

The values of Q_m and K_L, and of K_F and n, can be determined based on the intercept and slope of the plots of Eqs. (6) and (7), respectively, and are given in Table 2. The linear plots of the Langmuir and the Freundlich adsorption isotherms obtained at 25 °C are shown in Fig. 12a, b.

The adsorption data were well fitted by the Freundlich and Langmuir models (Table 2). However, the Freundlich model seemed to be more suitable than the Langmuir model, with an R^2 value of 0.9960. At the same time, the value of 1/n between 0.1 and 0.5 indicated that the adsorption of uranium by PE/PP-*g*-(PAAc-*co*-PAO) was a favorable adsorption process.

3.6 Simulated radioactive effluent adsorption

The pH value of the initial solution is considered to be an important parameter in the adsorption process [43, 44]. Since radioactive wastewater generally contains acid and inorganic salts [45], the adsorption capacity of uranium in simulated radioactive effluent was studied at pH values from 1 to 10, to which 30 g/L NaF was added. Figure 13 shows the removal ratio of uranium for the low initial concentrations of 10 and 100 μg/L, respectively, at various pH values from 1 to 10. With a decrease in pH value, the removal ratio of uranium decreased from 93.1 to 65.0%. After adsorption, the equilibrium concentrations of uranium were 0.7 and 3.5 μg/L. At lower pH values, the protonation of the adsorbents led to the generation of positive charge, which hindered the diffusion of uranium to the adsorbents. In spite of this, the PE/PP-*g*-(PAAc-*co*-PAO) adsorbent could remove 65% of uranium in the simulated radioactive effluent at pH 1.0. The adsorption capacity was quite close to that for the lower initial concentration of 10 μg/L. With the decrease in the pH value, the removal ratio of uranium also decreased from 93.0 to 71.2%. After adsorption, the equilibrium concentrations of uranium were 0.7 and 2.9 μg/L. These results indicated that the PE/PP-*g*-(PAAc-*co*-PAO) adsorbent can be used for radioactive effluent over a wide pH range, especially in the effluent polishing of uranium contaminants.

4 Conclusion

The commercially available and relatively inexpensive PE/PP fiber served as a substrate material for the preparation of a new adsorbent for the adsorption of uranium from aqueous solution. Poly-AAc and poly-AN chains were grafted onto the PE-coated PP skin–core fiber (PE/PP) by pre-irradiation-induced graft polymerization, followed by amidoximation to obtain the low-cost PE/PP-*g*-(PAAc-*co*-PAO) adsorbent, as demonstrated by FT-IR spectroscopy, XPS data, and SEM images. The good affinity and selectivity for uranium were achieved through the complexation of metal ions by AO groups on the PE/PP-*g*-(PAAc-*co*-PAO) fibers. The uranium adsorption capacity was 2.27 mg/g-adsorbent after 24 h in simulated seawater, and the equilibrium data were described well by the Freundlich isotherm model. The adsorption–desorption results indicated that the PE/PP-*g*-(PAAc-*co*-PAO) adsorbent can

Table 2 Isotherm parameters for the adsorption of uranium on the PE/PP-*g*-(PAAc-*co*-PAO) adsorbent

Isotherm model	Langmuir			Freundlich		
T (°C)	Q_m (mg/g)	K_L (L/mg)	R^2	K_F (mg/g) (L/mg)$^{1/n}$	1/n	R^2
25	124.38	1.06	0.9626	54.62	0.302	0.9960

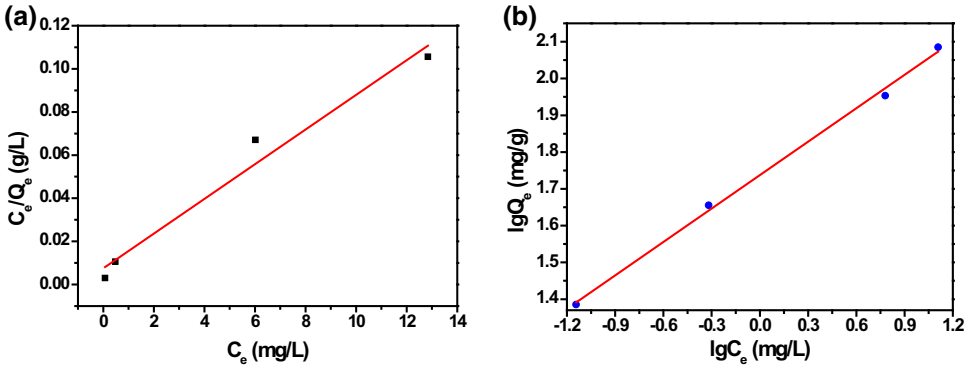

Fig. 12 Langmuir (**a**) and Freundlich (**b**) isotherms for uranium adsorption by the PE/PP-*g*-(PAAc-*co*-PAO) adsorbent

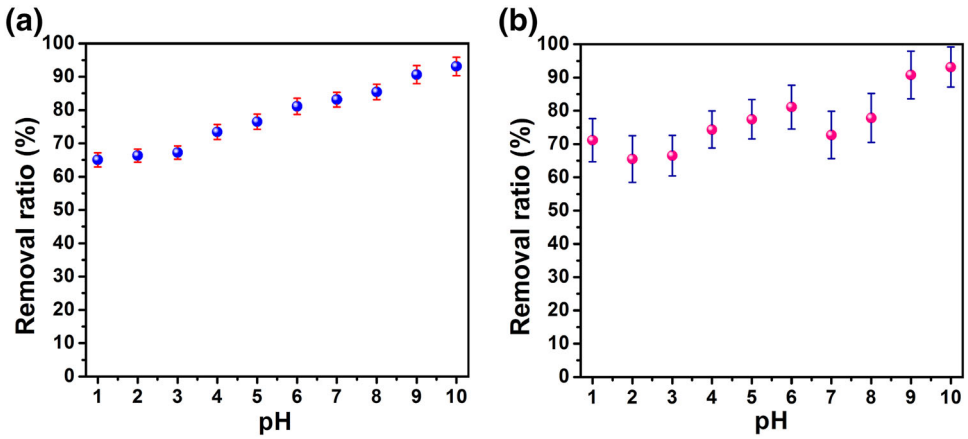

Fig. 13 Removal ratio of uranium with initial concentrations of 100 (**a**) and 10 μg/L uranium (**b**) at various pH values

be repeatedly used for at least five cycles with good adsorption performance. This study will reduce the production costs of the PE/PP-*g*-(PAAc-*co*-PAO) fibrous adsorbent at a large scale and of commercialized uranium extraction in the future. The PE/PP-*g*-(PAAc-*co*-PAO) adsorbent can be used over a wide range of pH values and in low-concentration uranium solutions from radioactive effluents. In 100 and 10 μg/L uranium solutions with pH values in the range 1.0–10.0, it showed high adsorption efficiency, with the maximum removal ratio reaching 93.1% and 93.0%, respectively. Therefore, the PE/PP-*g*-(PAAc-*co*-PAO) adsorbent can be applied as a cost-effective and efficient material for extracting uranium from aqueous solutions.

References

1. J. Zeng, H. Zhang, Y. Sui et al., New amidoxime-based material TMP-*g*-AO for uranium adsorption under seawater conditions. Ind. Eng. Chem. Res. **56**, 5021–5032 (2017). https://doi.org/10.1021/acs.iecr.6b05006
2. R.T. Mayes, J. Górka, S. Dai, Impact of pore size on the sorption of uranyl under seawater conditions. Ind. Eng. Chem. Res. **55**, 4339–4343 (2016). https://doi.org/10.1021/acs.iecr.5b03698
3. N. Seko, A. Katakai, S. Hasegawa et al., Aquaculture of uranium in seawater by a fabric-adsorbent submerged system. Nucl. Technol. **144**, 274–278 (2003). https://doi.org/10.13182/NT03-2
4. S.D. Alexandratos, X. Zhu, M. Florent et al., Polymer-supported bifunctional amidoximes for the sorption of uranium from seawater. Ind. Eng. Chem. Res. **55**, 4208–4216 (2016). https://doi.org/10.1021/acs.iecr.5b03742
5. Q. Gao, J. Hu, R. Li et al., Radiation synthesis of a new amidoximated UHMWPE fibrous adsorbent with high adsorption selectivity for uranium over vanadium in simulated seawater. Radiat. Phys. Chem. **122**, 1–8 (2016). https://doi.org/10.1016/j.radphyschem.2015.12.023
6. H.B. Pan, L.J. Kuo, C.M. Wai et al., Elution of uranium and transition metals from amidoxime-based polymer adsorbents for sequestering uranium from seawater. Ind. Eng. Chem. Res. **55**, 4313–4320 (2015). https://doi.org/10.1021/acs.iecr.5b03307
7. H.I. Lee, J.H. Kim, J.M. Kim et al., Application of ordered nanoporous silica for removal of uranium ions from aqueous solutions. J. Nanosci. Nanotechnol. **10**, 217–221 (2010). https://doi.org/10.1166/jnn.2010.1498
8. S. Duan, X. Liu, Y. Wang et al., Plasma surface modification of materials and their entrapment of water contaminant: a review. Plasma Process. Polym. **14**, 1600218 (2017). https://doi.org/10.1002/ppap.201600218
9. S. Duan, X. Xu, X. Liu et al., Highly enhanced adsorption performance of U (VI) by non-thermal plasma modified magnetic Fe_3O_4 nanoparticles. J. Colloid Interface Sci. **513**, 92–103 (2018). https://doi.org/10.1016/j.jcis.2017.11.008
10. H. Yu, S. Yang, H. Ruan et al., Recovery of U(VI) solutionss from simulated seawater with palygorskite/amidoxime polyacrylonitrile composite. Appl. Clay Sci. **111**, 67–75 (2015). https://doi.org/10.1016/j.clay.2015.01.035

11. W. Li, L.D. Troyer, S.S. Lee et al., Engineering nanoscale iron oxides for uranyl sorption and separation: optimization of particle core size and bilayer surface coatings. ACS. Appl. Mater. Interface **9**, 13163–13172 (2017). https://doi.org/10.1021/acsami.7b01042
12. H.S. Zhu, S.X. Duan, L. Chen et al., Plasma-induced grafting of acrylic acid on bentonite for the removal of U(VI) from aqueous solution. Plasma Sci. Technol. **19**, 115501 (2017). https://doi.org/10.1088/2058-6272/aa8168
13. M. Kanno, Present status of study on extraction of uranium from sea-water. J. Nucl. Sci. Technol. **21**, 1–9 (1984). https://doi.org/10.3327/jnst.21.1
14. W.J. Williams, A.H. Gillam, Separation of uranium from seawater by adsorbing colloid flotation. Analyst **103**, 1239–1243 (1978). https://doi.org/10.1039/AN9780301239
15. L.C. Tan, Q. Liu, X.Y. Jing et al., Removal of uranium(VI) ions from aqueous solution by magnetic cobalt ferrite/multiwalled carbon nanotubes composites. Chem. Eng. J. **273**, 307–315 (2015). https://doi.org/10.1016/j.cej.2015.01.110
16. L.C. Tan, J. Wang, Q. Liu et al., Facile preparation of oxine functionalized magnetic Fe_3O_4 particles for enhanced uranium(VI) adsorption. Colloids Surf. A **466**, 85–91 (2015). https://doi.org/10.1016/j.colsurfa.2014.11.020
17. T. Kawai, K. Saito, K. Sugita et al., Comparison of amidoxime adsorbents prepared by cografting methacrylic acid and 2-hydroxyethyl methacrylate with acrylonitrile onto polyethylene. Ind. Eng. Chem. Res. **39**, 2910–2915 (2000). https://doi.org/10.1021/ie990474a
18. Z. Xing, J.T. Hu, M.H. Wang et al., Properties and evaluation of amidoxime-based UHMWPE fibrous adsorbent for extraction of uranium from seawater. Sci. China Chem. **56**, 1504–1509 (2013). https://doi.org/10.1007/s11426-013-5002-x
19. H.H. Zhao, X.Y. Liu, M. Yu et al., A study on the degree of amidoximation of polyacrylonitrile fibers and its effect on their capacity to adsorb uranyl ions. Ind. Eng. Chem. Res. **54**, 3101–3106 (2015). https://doi.org/10.1021/ie5045605
20. S.Y. Xie, X.Y. Liu, B.W. Zhang et al., Electrospun nanofibrous adsorbents for uranium extraction from seawater. J. Mater. Chem. A **3**, 2552–2558 (2015). https://doi.org/10.1039/C4TA06120A
21. C. Gunathilake, J. Gorka, S. Dai et al., Amidoxime-modified mesoporous silica for uranium adsorption under seawater conditions. J. Mater. Chem. A **3**, 11650–11659 (2015). https://doi.org/10.1039/C5TA02863A
22. A. Zhang, G. Uchiyama, T. Asakura, Dynamic-state adsorption and elution behaviour of uranium(VI) ions from seawater by a fibrous and porous adsorbent containing amidoxime chelating functional groups. Adsorpt. Sci. Technol. **21**, 761–773 (2003). https://doi.org/10.1260/026361703773581812
23. L.J. Kuo, C.J. Janke, J.R. Wood et al., Characterization and testing of amidoxime-based adsorbent materials to extract uranium from natural seawater. Ind. Eng. Chem. Res. **55**, 4285–4293 (2015). https://doi.org/10.1021/acs.iecr.5b03267
24. S. Das, C. Tsouris, C. Zhang et al., Enhancing uranium uptake by amidoxime adsorbent in seawater: an investigation for optimum alkaline conditioning parameters. Ind. Eng. Chem. Res. **55**, 4294–4302 (2015). https://doi.org/10.1021/acs.iecr.5b02735
25. Y. Oyola, S. Vukovic, S. Dai, Elution by Le Chatelier's principle for maximum recyclability of adsorbents: applied to polyacrylamidoxime adsorbents for extraction of uranium from seawater. Dalton Trans. **45**, 8532–8540 (2016). https://doi.org/10.1039/C6DT00347H
26. T. Saito, S. Brown, S. Chatterjee et al., Uranium recovery from seawater: development of fiber adsorbents prepared via atom-transfer radical polymerization. J. Mater. Chem. A **2**, 14674–14681 (2014). https://doi.org/10.1039/C4TA03276D
27. H.B. Pan, L.J. Kuo, J. Wood et al., Towards understanding KOH conditioning of amidoxime-based polymer adsorbents for sequestering uranium from seawater. RSC. Adv. **5**, 100715–100721 (2015). https://doi.org/10.1039/C5RA14095A
28. N. Seko, A. Katakai, M. Tamada et al., Fine fibrous amidoxime adsorbent synthesized by grafting and uranium adsorption-elution cyclic test with seawater. Sep. Sci. Technol. **39**, 3753–3767 (2004). https://doi.org/10.1081/SS-200042997
29. M. Tamada. Current status of technology for collection of uranium from seawater. JAEA (2009). https://doi.org/10.1142/9789814327503_0026
30. R.V. Reis, A. Zydney, Bioprocess membrane technology. J. Membr. Sci. **297**, 16–50 (2007). https://doi.org/10.1016/j.memsci.2007.02.045
31. G.A. Tularam, M. Ilahee, Environmental concerns of desalinating seawater using reverse osmosis. J. Environ. Monit. **9**, 805–813 (2007). https://doi.org/10.1039/B708455M
32. H.J. Schenk, L. Astheimer, E.G. Witte et al., Development of sorbers for the recovery of uranium from seawater. 1. Assessment of key parameters and screening studies of sorber materials. Sep. Sci. Technol. **17**, 1293–1308 (1982). https://doi.org/10.1080/01496398208056103
33. J. Kim, C. Tsouris, Y. Oyola et al., Uptake of uranium from seawater by amidoxime-based polymeric adsorbent: field experiments, modeling, and updated economic assessment. Ind. Eng. Chem. Res. **53**, 6076–6083 (2014). https://doi.org/10.1021/ie4039828
34. J. Kim, Y. Oyola, C. Tsouris et al., Characterization of uranium uptake kinetics from seawater in batch and flow-through experiments. Ind. Eng. Chem. Res. **52**, 9433–9440 (2013). https://doi.org/10.1021/ie400587f
35. J. Hu, H. Ma, Z. Xing et al., Preparation of amidoximated ultrahigh molecular weight polyethylene fiber by radiation grafting and uranium adsorption test. Ind. Eng. Chem. Res. **55**, 4118–4124 (2015). https://doi.org/10.1021/acs.iecr.5b03175
36. H. Ma, H. Chi, J. Wu et al., A novel avenue to gold nanostructured microtubes using functionalized fiber as the ligand, the reductant, and the template. ACS. Appl. Mater. Interface **5**, 8761–8765 (2013). https://doi.org/10.1021/am402574b
37. X. Liu, J. Ao, X. Yang et al., Green and efficient synthesis of an adsorbent fiber by preirradiation-induced grafting of PDMAEMA and its Au(III) adsorption and reduction performance. J. Appl. Polym. Sci. **134**, 44955 (2017). https://doi.org/10.1002/app.44955
38. R. Li, H. Ma, Z. Xing et al., Synergistic effects of different comonomers on the uranium adsorption performance of amidoximated polyethylene nonwoven fabric in natural seawater. J. Radioanal. Nucl. Chem. **315**, 111–117 (2018). https://doi.org/10.1007/s10967-017-5639-6
39. R. Li, L. Pang, H. Ma et al., Optimization of molar content of amidoxime and acrylic acid in UHMWPE fibers for improvement of seawater uranium adsorption capacity. J. Radioanal. Nucl. Chem. **311**, 1771–1779 (2017). https://doi.org/10.1007/s10967-016-5117-6
40. A.R. Horrocks, J. Zhang, M.E. Hall, Flammability of polyacrylonitrile and its copolymers II. Thermal behaviour and mechanism of degradation. Polym. Int. **33**, 303–314 (1994). https://doi.org/10.1002/pi.1994.210330310
41. C. Ling, X. Liu, X. Yang et al., Uranium adsorption tests of amidoxime-based ultrahigh molecular weight polyethylene fibers in simulated seawater and natural coastal marine seawater from different locations. Ind. Eng. Chem. Res. **56**, 1103–1111 (2017). https://doi.org/10.1021/acs.iecr.6b04181
42. T. Suzuki, K. Saito, T. Sugo et al., Fractional elution and determination of uranium and vanadium adsorbed on amidoxime fiber

from seawater. Anal. Sci. **16**, 429–432 (2000). https://doi.org/10.2116/analsci.16.429

43. A. Zhang, G. Uchiyama, T. Asakura, pH Effect on the uranium adsorption from seawater by a macroporous fibrous polymeric material containing amidoxime chelating functional group. React. Funct. Polym. **63**, 143–153 (2005). https://doi.org/10.1016/j.reactfunctpolym.2005.02.015
44. N. Horzum, T. Shahwan, O. Parlak et al., Synthesis of amidoximated polyacrylonitrile fibers and its application for sorption of aqueous uranyl ions under continuous flow. Chem. Eng. J. **213**, 41–49 (2012). https://doi.org/10.1016/j.cej.2012.09.114
45. N.K. Sethy, R.M. Tripathi, V.N. Jha et al., Assessment of natural uranium in the ground water around jaduguda uranium mining complex. India J. Environ. Prot. Ecol. **2**, 1002 (2011). https://doi.org/10.4236/jep.2011.27115